



Article

Exploration of Defect Dynamics and Color Center Qubit Synthesis with Pulsed Ion Beams

Thomas Schenkel ^{1,*}, Walid Redjem ², Arun Persaud ¹, Wei Liu ¹, Peter A. Seidl ¹, Ariel J. Amsellem ¹, Boubacar Kanté ² and Qing Ji ¹

- Accelerator Technology and Applied Physics Division, Lawrence Berkeley National Laboratory, Berkeley, CA 94720, USA; apersaud@lbl.gov (A.P.); weiliu01@lbl.gov (W.L.); paseidl@lbl.gov (P.A.S.); ajamsellem@lbl.gov (A.J.A.); qji@lbl.gov (Q.J.)
- Department of Electrical Engineering and Computer Science, University of California, Berkeley, CA 94720, USA; wredjem@berkeley.edu (W.R.); bkante@berkeley.edu (B.K.)
- * Correspondence: t_schenkel@lbl.gov

Abstract: Short-pulse ion beams have been developed in recent years and now enable applications in materials science. A tunable flux of selected ions delivered in pulses of a few nanoseconds can affect the balance of defect formation and dynamic annealing in materials. We report results from color center formation in silicon with pulses of 900 keV protons. G-centers in silicon are near-infrared photon emitters with emerging applications as single-photon sources and for spin-photon qubit integration. G-centers consist of a pair of substitutional carbon atoms and one silicon interstitial atom and are often formed by carbon ion implantation and thermal annealing. Here, we report on G-center formation with proton pulses in silicon samples that already contained carbon, without carbon ion implantation or thermal annealing. The number of G-centers formed per proton increased when we increased the pulse intensity from 6.9×10^9 to 7.9×10^{10} protons/cm²/pulse, demonstrating a flux effect on G-center formation efficiency. We observe a G-center ensemble linewidth of 0.1 nm (full width half maximum), narrower than previously reported. Pulsed ion beams can extend the parameter range available for fundamental studies of radiation-induced defects and the formation of color centers for spin-photon qubit applications.

Keywords: pulsed ion beams; induction accelerator; photon emitters; qubits; color centers



Citation: Schenkel, T.; Redjem, W.; Persaud, A.; Liu, W.; Seidl, P.A.; Amsellem, A.J.; Kanté, B.; Ji, Q. Exploration of Defect Dynamics and Color Center Qubit Synthesis with Pulsed Ion Beams. *Quantum Beam Sci.* 2022, 6, 13. https://doi.org/ 10.3390/qubs6010013

Academic Editor: Takeshi Ohshima

Received: 30 December 2021 Accepted: 1 March 2022 Published: 16 March 2022

Publisher's Note: MDPI stays neutral with regard to jurisdictional claims in published maps and institutional affiliations.



Copyright: © 2022 by the authors. Licensee MDPI, Basel, Switzerland. This article is an open access article distributed under the terms and conditions of the Creative Commons Attribution (CC BY) license (https://creativecommons.org/licenses/by/4.0/).

1. Introduction

Ion beams are very widely used in the fabrication of classical semiconductor devices [1]. In recent years, quantum information science [2] has emerged from a topic of basic research towards increasing the number of applications that show quantum advantages in sensing, communications, and computing. The formation and integration of some promising qubit candidates such as donor spins and color centers [3–5] can be accomplished using ion beams

In the development of ion beams, short-pulse ion beams from induction linear accelerators (LINACs) [6] and from laser-plasma acceleration have recently become available for materials studies [7,8]. When a desired fluence of ions (ions/cm 2) is delivered, the flux (ions/cm 2 /s) and the pulse length (e.g., 0.1 to 10 ns) can affect the balance of defect formation and dynamic annealing [9] in ion–solid interactions.

The spins of donor atoms in silicon and other semiconductors are promising qubit candidates, where the fabrication finesse of end-of-roadmap silicon technologies can be applied for qubit integration [5,10]. Color centers, such as the nitrogen-vacancy center in diamond, are already widely used for quantum sensing [11] and emerging quantum communication applications [12]. Recently, color centers and optically active defects in silicon have been revisited for quantum applications, and single near-infrared emitters, such as G-centers [12] and W-centers, have been characterized [13]. In the formation of dopant

Quantum Beam Sci. 2022, 6, 13 2 of 9

and color center qubits with ion beams and conventional fabrication techniques, increased qubit formation efficiencies have been achieved in recent years which have enabled many qubit physics demonstrations and proof-of-concept experiments with increasing degrees of qubit control and complexity [10,14,15]. In studies of G-centers in silicon, the centers have often been formed by carbon ion implantation, followed by thermal annealing [12,16]. In this process, substitutional carbon atom pairs are formed in the thermal annealing step from the implanted carbon ions. The thermal annealing step also repairs the implant damage from the carbon ion implantation and some silicon interstitials can diffuse to carbon atom pairs to form G-centers [12]. Silicon interstitials can also be formed by irradiation with MeV protons [16]. The development of intense and tunable ion pulses opens new opportunities for the exploration of the fundamental defect dynamics of radiation-induced defects, defect engineering, and qubit synthesis far from equilibrium.

2. Materials and Methods

Pulsed ion beams can be formed through time-dependent deflection or chopping of conventional ion beams without beam compression [9]. However, much higher peak currents can be achieved with induction accelerators [6], pulsed single-gap-type accelerators [17,18], and laser-plasma acceleration of ions [7]. In the following we present results from NDCX-II (Neutralized Drift Compression Experiment-II), an ion induction linear accelerator at Berkeley Lab [6]. The technology of ion induction accelerators with drift compression has been developed in the context of heavy ion fusion driver development and for high energy density science experiments [19]. The dynamics of radiation-induced defects can become accessible in pump-probe type experiments when the interaction time is controlled with short ion pulses. In the current configuration, NDCX-II delivers 1 MeV protons and helium ions with peak currents of up to 2 A, and beam spots of 3 to 10 mm². A photo and a schematic of the ~12 m long accelerator are shown in Figure 1. Ions are injected from a multi-cusp plasma ion source with an injection energy of typically 100 to 140 keV. The ion source delivers about 1µs pulses of helium ions from an array of about 1900 densely packed beams that are formed in a plasma ion source and extracted from high transmission grids across an extraction area with a diameter of 60 mm [20]. The beams merge into a single beam with a peak current of up to 150 mA, which is then accelerated and compressed in the linear accelerator.

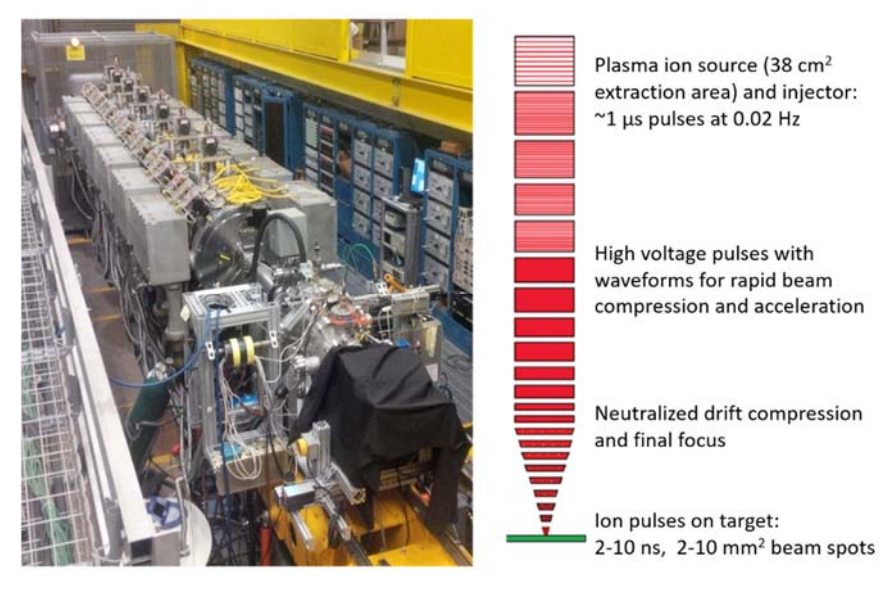


Figure 1. Photo of NDCX-II, an ion induction LINAC at Berkeley Lab [6,19], and an illustration of its operating principles for the formation of ns ion pulses by neutralized drift compression.

Ions are then subjected to pulsed electrical fields in induction cells designed to accelerate the pulse to the final energy of up to 1.1 MeV, to shape the ion pulse velocity distribution

Ouantum Beam Sci. 2022, 6, 13 3 of 9

and to enable drift compression of the ion pulse. Longitudinal pulse compression is mainly accomplished in drift sections where faster ions catch up with slower ions within the ion pulse from the engineered velocity tilt. A beam radius of a few cm is maintained with a series of 28 pulsed solenoids. After the last acceleration gap, the final drift compression of the space-charge-dominated ion bunch requires the injection of electrons to compensate space-charge forces that would otherwise limit the minimum pulse duration at the target. The last focusing element is a pulsed solenoid magnet (up to 7 T) that focuses the beam to spots with diameters of ~1.5 to 10 mm, depending on the field strength. Ion pulses are thus compressed longitudinally, (in pulse length) from ~1 µs to 2 ns, and laterally, i.e., the spatial focusing domain, from 60 mm to ~2 mm, to reach peak intensities of up to ~60 A/cm². The final ion kinetic energy spread is typically $\pm 8\%$. The accelerator lattice can be tuned with particle-in-cell codes such as WarpX [21] (and with emerging machine learning tools) to select a range of fluences and flux conditions for studies of the defect dynamics and radiation effects in semiconductor devices [22]. For target irradiations, the ion energy at NDCX-II can be tuned from as low as 100 keV, for a coasting beam from the injector, up to 1.1 MeV, with optimal waveforms and acceleration in the currently available induction cells. To date, proton and helium ion pulses have been formed with a multi-cusp plasma ion source [20]. The beams of other ion species can also be formed since the ion source is very versatile. Previously we had used Li⁺ surface-emission-type ion sources, which have the advantage of lower emittance and higher source brightness [6,19]. However, these lithium sources suffered from short lifetimes and much higher service requirements compared to the plasma ion sources we now use. Helium ion pulses at 1.1 MeV with a 2.1-A peak current, a pulse duration of 2.4 ns (FWHM), and a beam spot size of 1.5 mm FHWM have been reported [22]. The corresponding flux was $\sim 2 \times 10^{11}$ ions/cm²/pulse, or 10^{20} ions/cm²/s at the peak of the pulse waveform.

In earlier studies of radiation effects on pnp silicon transistors with 1 MeV helium ions, we found that the damage rate per ion in a Messenger–Spratt-type damage rate analysis was the same for helium ion irradiation with conventional ion beams (~1 to 100 $\mu A/cm^2$, or ~6 \times 10³ to 6 \times 10⁵ ions/cm²/ns) and pulsed ion beams that delivered ions at a flux of 2.5 \times 10° He/cm²/ns (with a pulse length of 10 ns), i.e., at a dose rate that that was over a thousand times higher [22]. Increasing the flux to >10¹0 ions/cm²/ns can lead to deviations of low flux and high flux damage rates in silicon diodes. Proton pulses from NDCX-II have been used to calibrate radiochromic films that are widely used to quantify the intensity, energy, and angular distributions of high energy proton pulses in laser-plasma acceleration experiments [7,8]. Peak radiation doses reached up to 100 kGy in 10 ns pulses, or 7 \times 10¹¹ Gy/s for proton intensities of up to 2 \times 10¹¹0 protons/cm²/ns at a kinetic energy of 1 MeV [8]. Such high energy deposition rates also enable the exploration of dose rate effects on the biological effectiveness of energetic protons [23]. We summarize the performance parameters for NDCX-II in Table 1.

Table 1. List of NDCX-II parameters.

Performance Parameter	NDCX-II Parameter Value
Ion energy	0.1 to 1.1 MeV
Ion species	Protons, helium, higher Z species possible
Peak current	0.001 to 2 A
Pulse length (FWHM)	2 ns to 1 μs
Ions per pulse	~10 ⁸ to 10 ¹¹
Beam diameter on target	~1.5 to 10 mm
Pulse intensity	up to ~10 ¹² ions/cm ² /shot (to date)
Repetition rate	1 shot/45 s
Shots per day	up to ~500

Ouantum Beam Sci. 2022, 6, 13 4 of 9

When operating the plasma ion source with hydrogen gas for proton formation, H_2^+ ions are also formed and injected into the beamline, together with the protons [8]. In earlier experiments with 1.1 MeV protons, the H_2^+ ions were observed arriving about 600 ns after the main proton pulse [8]. In the current study, we wanted to avoid defect formation from H_2^+ ions, and we thus used a 4 µm thick aluminum foil to stop them; hence there is no H_2^+ peak in the 2 µs temporal window in Figure 2 (left). The double peak structure highlighted in Figure 2 (right) results from the velocity distribution of ions in the pulse. This feature can be increased or reduced by tuning the acceleration waveforms, and it can enable exploration of defect formation under double-pulse conditions. Using the SRIM code [24], we estimated that 1.1 MeV protons lost about 200 keV in the aluminum foil before reaching the silicon targets through 2 mm diameter apertures. The intensity of the pulse on the right in Figure 2 was $7.9 \pm 1.6 \times 10^{10}$ protons/cm².

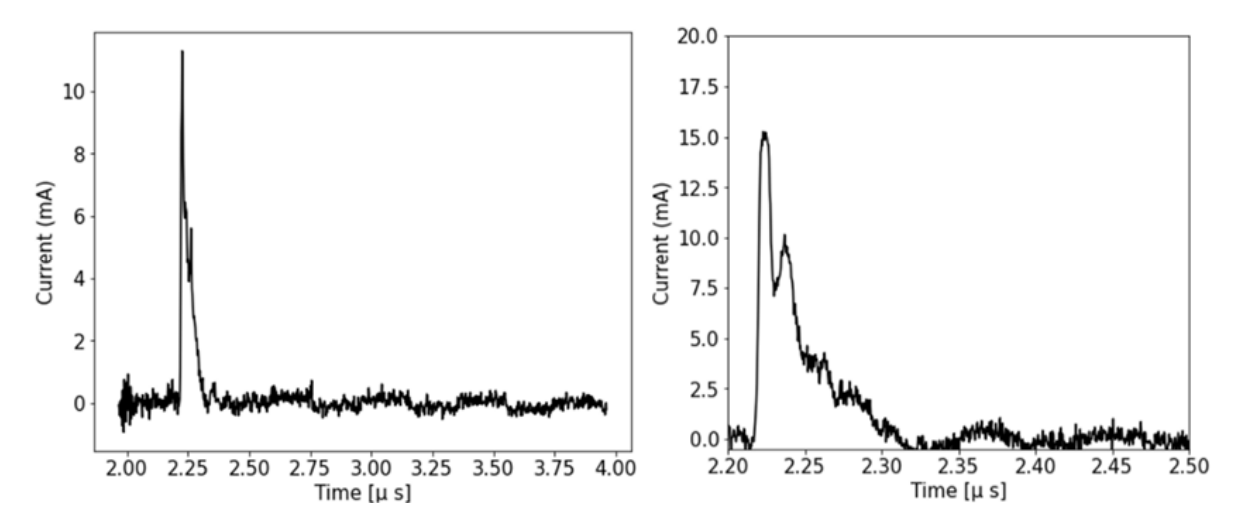


Figure 2. Examples of the proton pulses from NDCX-II used for G-center formation in silicon.

The interplay of damage formation and annealing in a single ion pulse depends on the ratio of elastic and inelastic energy loss processes, as well as on heating the sample lattice. For repeated pulses, excitations and heating can lead to damage accumulation and damaged annealing of defects formed by a series of ion impacts in a selected spatiotemporal window. The ability to tune the ion flux with nanosecond pulses now opens a rich field of defect engineering and exploration of defect dynamics with pulsed ion beams. Flux, or dose rate effects, have been observed for many years using conventional ion beams of varying intensity [9]. Being able to control the ion pulse length on a ns time scale [25] now opens the possibility to tune ion pulses for the optimization of desired defects, such as color centers and spin-photon qubit candidates. Ion pulses from laser-plasma acceleration have complementary properties compared to those from NDCX-II, including higher ion intensities, multi-species composition, higher ion peak energies, and broad energy distributions [7,8].

For the irradiation studies, we used float zone silicon samples, with (111) crystal orientation and a resistivity of ~100 Ohm cm. Analysis by secondary ion mass spectrometry (SIMS, www.EAG.com, accessed on 28 December 2021) prior to irradiation showed a distribution of carbon atoms with a concentration of up to 10^{20} C/cm³ near the native oxide surface, which dropped to the SIMS sensitivity limit of 10^{16} C/cm³ at a depth of 150 nm (Figure 3). Integrating the very steep, near-surface depth distribution of the carbon concentration, we found that the corresponding carbon areal density was 2×10^{14} C/cm². The origin of this carbon in our silicon samples is likely extended storage in polymer-based wafer carriers. No carbon ion implantation or annealing were performed in the experiments we report on here. We selected this starting material because we wanted to see if we could form G-centers from carbon that was already present in the silicon samples. We can then

Quantum Beam Sci. 2022, 6, 13 5 of 9

also compare results to G-center ensemble properties from the standard process of carbon ion implantation and thermal annealing.

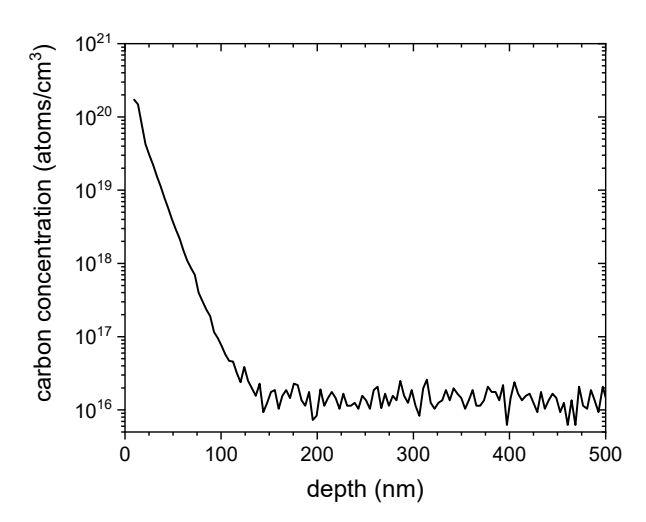


Figure 3. SIMS depth profile of the carbon in the silicon (111) samples used for G-center formation by proton irradiation. The carbon was present in the as-received silicon samples, and there was no carbon ion implantation step.

Photoluminescence spectra were recorded at 3 K using a scanning confocal microscope optimized for near-infrared spectroscopy. Optical excitation was performed with a 532 nm continuous laser focused onto the sample through a high-numerical-aperture microscope objective (NA = 0.85). The excitation power, measured at the entrance of the objective lens, was fixed at 1mW. The PL signal was collected by the same objective and directed to a spectrometer (900 to 1620 nm) coupled to an InGaAs camera (cooled to 193 K).

3. Results

For the study of G-center formation, we tuned proton pulses to flux levels of $6.9~(\pm 0.7)\times 10^9~$ and $7.9~(\pm 1.6)\times 10^{10}~$ protons/cm²/pulse, respectively (Figure 2). We determined the ion flux with Faraday cup measurements of a series of pulses before and after the pulse(s) that irradiated a sample. Ion beam spots were defined with a 2 mm diameter aperture, and we irradiated three or four spots separated by several mm on silicon samples (7 mm \times 7 mm) that had been cut from the Si (111) starting wafer material. We then conducted PL measurements to quantify light emission in the near-infrared spectral region from about 1200 nm to 1500 nm. The 532 nm excitation light used for PL can excite color centers over a depth of less than 1 μ m. To compare the PL intensity from several irradiated areas for a series of different irradiation conditions, we kept the laser excitation power constant and used the same diffraction limited focusing condition on the sample surface in the respective areas. In addition, the PL spectra have been normalized by taking the integration times for each measurement into account. Examples of near IR PL spectra taken at a temperature of 3 K are shown in Figure 4, where we focus on the spectra region from 1260 to 1320 nm.

The PL spectra in Figure 4 show that the emission from G-centers at 1278.56 nm is about 100% more intense for the one-shot sample at a flux of 7.9×10^{10} protons/cm²/pulse compared to the sample that had received ten shots at a lower flux of 6.9×10^9 protons/cm²/pulse. Meanwhile, the fluence for these two irradiations was higher by only 14% for the single high flux pulse vs. the ten lower flux pulses. The observation that the resulting G-center intensities differ for the high flux vs. low flux pulse conditions for similar proton fluences demonstrates a super-linear effect of the proton flux, or dose rate, on G-center formation. When we zoomed in on the emission line at 1278.56 nm from ensembles of G-centers that were formed for a series of irradiation conditions, as in Figure 4, we observed an ensemble line width distribution of 0.1 nm (FWHM). This ensemble linewidth is much narrower

Ouantum Beam Sci. 2022, 6, 13 6 of 9

than the linewidth observed in samples with G-center ensembles formed by carbon ion implantation and thermal annealing of about 0.4 nm [12,24]. The depth distribution of the G-centers observed here is not known, and we have not yet quantified the absolute number of G-centers.

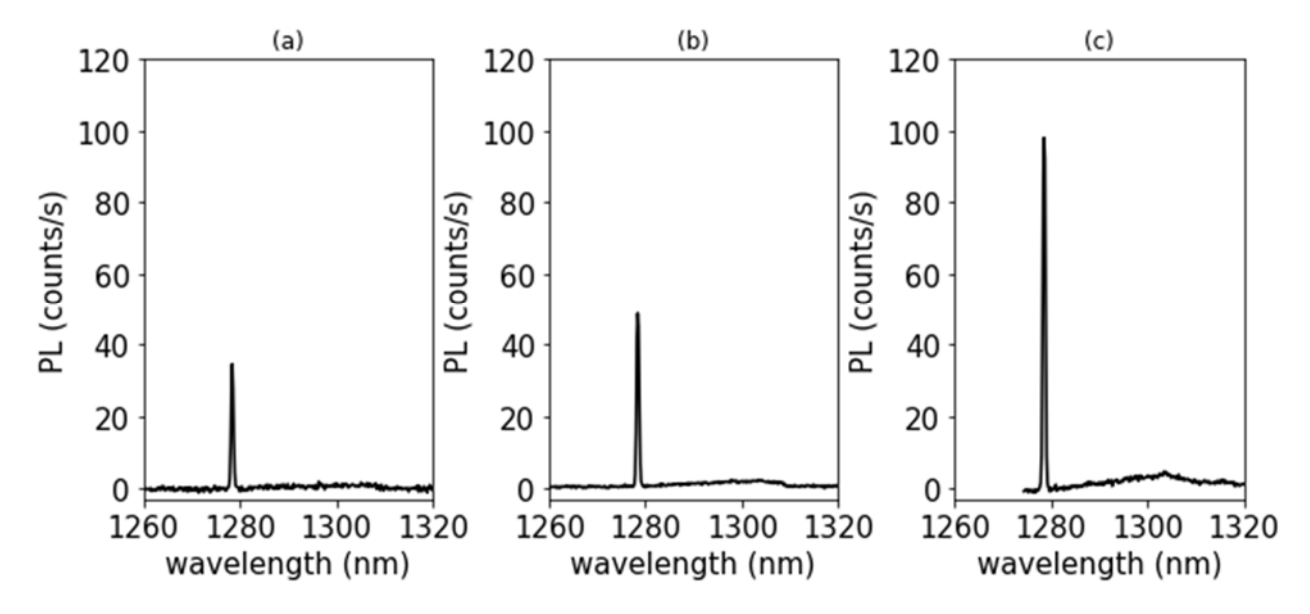


Figure 4. Near-IR photo-luminescent spectra collected at a sample temperature of 3 K from Si (111) samples that had received (a) one and (b) ten proton pulses at a flux of 6.9 (± 0.7) × 10^9 protons/cm²/pulse, and (c) one pulse at a flux of 7.9 (± 1.6) × 10^{10} protons/cm²/pulse. The relative intensities are normalized to the signal integration time for comparison.

4. Discussion

Dose rate effects, or flux effects on defect structures that develop resulting from the ion implantation of semiconductors have been observed for many years [9]. In our example, we observe a super-linear scaling of G-center formation with proton flux, and we control the proton pulse length on the 10 ns time scale. The range of 900 keV protons in silicon estimated from SRIM [25] is about 14 μm . Vacancies and interstitials are formed in elastic collisions at a rate of about 2 \times 10 $^{-4}$ damage events/proton/nm in the top 1 μm of the samples, or 0.2 damage events/proton/ μm . Silicon interstitials can migrate over tens of nanometers following damage events [9]. The clustering of silicon interstitials from overlapping damage cascades could lead to the formation of many defect structures, including W-centers, which we did not observe. Increased clustering and the formation of extended defects can be explored with helium and heavier ion species.

We estimated the maximum temperature increase due to the proton pulse based on the energy loss of protons in silicon (which we estimated using the SRIM code [24]), together with the proton fluence values in our irradiations and a value for the specific heat of silicon of 0.7 J/g/K. We found that at a 7.9×10^{10} protons/cm²/pulse, the maximum temperature increase from the proton energy deposition in the silicon sample was very low, only about 4 K at a depth of 0.5 μm .

To understand the underlying mechanisms responsible for the flux effect on G-center formation, detailed simulations could track the energy deposition and the spatio-temporal dynamics of target excitation and heating, together with elastic collisions, damage cascade expansion and cooling, and the movement of silicon interstitials and vacancies.

Silicon interstitials can combine with two substitutional carbon atoms to form a G-center [16,26]. Multi-scale simulations of radiation damage and defect formation [27] would have to track a time scale from ps to ms and length scales from sub-nm to the diffusion length of silicon interstitials of tens of nanometers [9]. By changing the rate at which ions impinge on the silicon sample, we can adjust the probability that defects induced by one

Ouantum Beam Sci. 2022, 6, 13 7 of 9

proton can interact with defects from the next proton that impinge in the same area. The ion pulse length constrains this time window to a few nanoseconds. A proton intensity of ~ 10^{10} protons/cm² constrains the interaction window to an average distance between proton impacts of about 100 nm. Repeated pulses can lead to the accumulation of defects and color centers, but consecutive pulses can also anneal or alter the defects that had been formed in an earlier pulse. The instantaneous energy deposition in a more intense, higherflux proton or ion pulse leads to increased transient excitations and lattice heating and can affect the mobility of interstitials and vacancies. G-centers formed here were observed for relatively high fluxes and relatively low fluences of MeV protons, < 10^{11} protons/cm², compared to some earlier studies (> 10^{13} protons/cm²) [12,24]. Comparing the absolute formation efficiency of G-centers for different processing methods is difficult because the presence of substitutional carbon atom pairs is a prerequisite of G-center formation. While the concentration of carbon can be readily quantified, e.g., by SIMS, the lattice positions and coordination of carbon atoms and pairs of carbon atoms is harder to assess.

The observation of a narrow linewidth of 0.1 nm in the G-center ensembles formed indicates that the high proton flux does not lead to the accumulation of other radiation induced defects, such as vacancy clusters, which could lead to inhomogeneous broadenings of G-center line widths. Further, these narrow linewidth ensembles are formed from carbon that was likely introduced by a surface contamination process during the extended storage of wafers in polymer-based wafer carriers. The comparison to G-center ensembles from carbon ion implantation and thermal annealing shows that the ion implant process likely leads to residual lattice damage after thermal annealing that causes broader G-center ensemble line widths.

With the access to single color centers demonstrated in materials such as diamond, silicon carbide, and silicon, color centers have become available for applications in quantum information science and technology. Studies of (single) color centers can also be used to probe the fundamental aspects of the dynamics of radiation-induced defects, complementing other well-established ensemble methods such as ion beam-induced charge collection and deep-level-transient spectroscopy [28].

5. Conclusions

Pulsed ion beams from induction LINACs can deliver tunable intensities of protons and heavier ions to targets in nanosecond pulses with peak flux levels of ~ 10^9 to 10^{12} ions/cm²/pulse. Flux conditions can be tuned to affect the balance of damage formation and dynamic annealing in materials such as semiconductors. This control of the ion pulse length constrains the temporal window for defect interactions in single pulses and enables studies on the formation and annealing dynamics of radiation-induced defects. We reported results from G-center formation in carbon-doped silicon with pulsed proton beams. We observed that the number of G-centers formed per proton increased when we increased the pulse intensity from 6.9×10^9 to 7.9×10^{10} protons/cm²/pulse. This demonstrates a flux effect on color center formation efficiency. Pulsed ion beams can extend the parameter range for defect engineering and the exploration of color center qubit synthesis beyond the range of conventional ion beams.

Author Contributions: T.S. led the study; W.R. and B.K. conducted photoluminescence measurements; A.P., W.L. and Q.J. conducted the irradiations; P.A.S. and A.J.A. contributed to data analysis, data interpretation and writing of the manuscript; All authors contributed to data analysis, data interpretation, and the writing of the manuscript. All authors have read and agreed to the published version of the manuscript.

Funding: Work at LBNL was supported by the Office of Science and Office of Fusion Energy Sciences of the U.S. Department of Energy, and by Laboratory Directed Research and Development (LDRD) funding from Berkeley Lab provided by the Director, Office of Science, of the U.S. Department of Energy under Contract No. DE-AC02-05CH11231. Work at the Molecular Foundry was supported by the Office of Science, Office of Basic Energy Sciences, of the U.S. Department of Energy under

Ouantum Beam Sci. 2022. 6.13

Contract No. DE-AC02-05CH11231. BK acknowledges funding through the NSF QLCI program through grant number OMA-2016245 and the NSF QuIC-TAQS through award number 2137645.

Institutional Review Board Statement: Not applicable.

Informed Consent Statement: Not applicable.

Data Availability Statement: Raw data can be made available upon reasonable request.

Acknowledgments: We gratefully acknowledge support of this work through the coordinated research project "F11020" of the International Atomic Energy Agency (IAEA). We thank Takeshi Katayanagi for technical support.

Conflicts of Interest: The authors declare no conflict of interest.

References

- 1. Poate, J.M.; Saadatmand, K. Ion beam technologies in the semiconductor world. Rev. Sci. Instrum. 2002, 73, 868. [CrossRef]
- 2. Nielson, M.A.; Chuang, I.L. Quantum Computing and Quantum Information; Cambridge University Press: Cambridge, UK, 2000.
- Kane, B.A. A silicon-based nuclear spin quantum computer. Nature 1998, 393, 133. [CrossRef]
- Toyli, D.M.; Weis, C.D.; Fuchs, G.D.; Schenkel, T.; Awschalom, D.D. Chip-Scale Nanofabrication of Single Spins and Spin Arrays in Diamond. Nano Lett. 2010, 10, 3168. [CrossRef] [PubMed]
- 5. Ilg, M.; Weis, C.D.; Schwartz, J.; Persaud, A.; Ji, Q.; Lo, C.C.; Bokor, J.; Hegyi, A.; Guliyev, E.; Rangelow, I.W.; et al. Improved single ion implantation with scanning probe alignment. *J. Vac. Sci. Technol. B* **2012**, *30*, 06FD04. [CrossRef]
- 6. Seidl, P.A.; Persaud, A.; Stettler, M.; Takakuwa, J.H.; Waldron, W.L.; Schenkel, T.; Barnard, J.J.; Friedman, A.; Grote, D.P.; Davidson, R.C.; et al. Short intense ion pulses for materials and warm dense matter research. *Nucl. Instrum. Methods Phys. Res. Sect. A* 2015, 800, 98. [CrossRef]
- 7. Steinke, S.; Bin, J.H.; Park, J.; Ji, Q.; Nakamura, K.; Gonsalves, A.J.; Bulanov, S.S.; Thévenet, M.; Toth, C.; Vay, J.-L.; et al. Acceleration of high charge ion beams with achromatic divergence by petawatt laser pulses. *Phys. Rev. Accel. Beams* **2020**, 23, 021302. [CrossRef]
- 8. Bin, J.H.; Ji, Q.; Seidl, A.; Rafrtrey, D.; Steinke, S.; Persaud, A.; Nakamura, K.; Gonsalves, S.; Leemand, W.P.; Schenkel, T. Absolute calibration of GafChromic film for very high flux laser driven ion beams. *Rev. Sci. Instrum.* **2019**, *90*, 053301. [CrossRef] [PubMed]
- 9. Wallace, J.B.; Charnvanichborikarn, S.; Bayu Aji, L.B.; Myers, M.T.; Shao, L.; Kucheyev, S.O. Radiation defect dynamics in Si at room temperature studied by pulsed ion beams. *J. Appl. Phys.* **2015**, *118*, 135709. [CrossRef]
- 10. McCallum, J.C.; Johnson, B.C.; Botzem, T. Donor-based qubits for quantum computing in silicon featured. *Appl. Phys. Rev.* **2021**, 8, 031314. [CrossRef]
- 11. Degen, C.L.; Reinhard, F.; Cappellaro, P. Quantum sensing. Rev. Mod. Phys. 2017, 89, 03500. [CrossRef]
- 12. Redjem, W.; Durand, A.; Herzig, T.; Benali, A.; Pezzagna, S.; Meijer, J.; Kuznetsov, A.Y.; Nguyen, N.S.; Cueff, S.; Gérard, J.-M.; et al. Single artificial atoms in silicon emitting at telecom wavelengths. *Nat. Electron.* **2020**, *3*, 738. [CrossRef]
- 13. Baron, Y.; Durand, A.; Udvarhelyi, P.; Herzig, T.; Khoury, M.; Pezzagna, S.; Meijer, J.; Robert-Philip, I.; Abbarchi, M.; Hartmann, J.-M.; et al. Detection of single W-centers in silicon. *arXiv* **2018**, arXiv:2108.04283.
- 14. Bienfait, A.; Pla, J.; Kubo, Y.; Zhou, X.; Stern, M.; Lo, C.C.; Weis, C.D.; Schenkel, T.; Vion, D.; Esteve, D.; et al. Controlling spin relaxation with a cavity. *Nature* **2016**, *531*, 74. [CrossRef] [PubMed]
- 15. Lühmann, T.; John, R.; Wunderlich, R.; Meijer, J.; Pezzagna, S. Coulomb-driven single defect engineering for scalable qubits and spin sensors in diamond. *Nat. Commun.* **2019**, *10*, 4956. [CrossRef] [PubMed]
- 16. Beaufils, C.; Redjem, W.; Rousseau, E.; Jacques, V.; Kuznetsov, A.Y.; Raynaud, C.; Voisin, C.; Benali, A.; Herzig, T.; Pezzagna, S.; et al. Optical properties of an ensemble of G-centers in silicon. *Phys. Rev. B* **2018**, *97*, 035303. [CrossRef]
- 17. Chu, W.K.; Mader, S.R.; Gorey, E.F.; Baglin, J.E.E.; Hodgson, R.T.; Neri, J.M.; Hammer, D.A. Pulsed ion beam irradiation of silicon. *Nucl. Instrum. Methods Phys. Res.* **1982**, *182*, 443. [CrossRef]
- 18. Bieniosek, F.M.; Celata, C.M.; Henestroza, E.; Kwan, J.W.; Prost, L.; Seidl, P.A.; Friedman, A.; Grote, D.P.; Lund, S.M.; Haber, I. 2-MV electrostatic quadrupole injector for heavy-ion fusion. *Phys. Rev. Spec. Top. Accel. Beams* **2005**, *8*, 010101. [CrossRef]
- 19. Barnard, J.J.; More, R.M.; Terry, M.; Friedman, A.; Henestroza, E.; Koniges, A.; Kwan, J.W.; Ng, A.; Ni, P.A.; Liu, W.; et al. NDCX-II target experiments and simulations. *Nucl. Instrum. Methods Phys. Res. Sect. A* **2014**, 733, 45. [CrossRef]
- 20. Ji, Q.; Seidl, P.A.; Waldron, W.L.; Takakuwa, J.; Friedman, A.; Grote, D.P.; Persaud, A.; Barnard, J.J.; Schenkel, T. Development and testing of a pulsed helium ion source for probing materials and warm dense matter studies. *Rev. Sci. Instrum.* **2016**, *87*, 02B707. [CrossRef] [PubMed]
- 21. Vay, J.-L.; Almgren, A.; Bell, J.; Ge, L.; Grote, D.P.; Hogan, M.; Kononenko, O.; Lehe, R.; Myers, A.; Ng, C.; et al. Warp-X: A new exascale computing platform for beam-plasma simulations. *Nucl. Instrum. Methods Phys. Res. Sect. A* **2018**, 909, 476. [CrossRef]
- 22. Schenkel, T.; Ludewigt, B.A.; Seidl, P.A.; Persaud, A.; Ji, Q.; Steinke, S.; Bulanov, S.S.; Leemans, W.P.; Bielejec, E.S.; Barnard, J.J.; et al. Short Intense Ion Pulses for Radiation Effects Research Using NDCX-II and BELLA-i. *J. Radiat. Eff. Res. Eng.* 2018, 36, 97.

Quantum Beam Sci. **2022**, 6, 13 9 of 9

23. Bin, J.; Obst-Huebl, L.; Mao, J.H.; Nakamura, K.; Geulig, L.D.; Chang, H.; Ji, Q.; He, L.; De Chant, J.; Kober, Z.; et al. A new platform for ultra-high dose rate radiobiological research using the BELLA PW laser proton beamline. *Sci. Rep.* 2022, 12, 1484. [CrossRef] [PubMed]

- 24. Interactions of Ions with Matter: SRIM-The Stopping and Range of Ions in Matter. Available online: www.srim.org (accessed on 28 December 2021).
- 25. Seidl, P.A.; Ji, Q.; Persaud, A.; Feinberg, E.; Ludewigt, B.; Silverman, M.; Sulyman, A.; Waldron, W.L.; Schenkel, T.; Barnard, J.J.; et al. Irradiation of materials with short, intense ion pulses at NDCX-II. *Laser Part. Beams* **2017**, *35*, 373. [CrossRef]
- 26. Udvarhelyi, P.; Somogyi, B.; Thiering, G.; Gali, A. Identification of a Telecom Wavelength Single Photon Emitter in Silicon. *Phys. Rev. Lett.* **2021**, 127, 196402. [CrossRef] [PubMed]
- 27. Hamedani, A.; Byggmastar, J.; Djurabekova, F.; Alahyarizadeh, G.; Ghaderi, R.; Minuchehr, A.; Nordlund, K. Primary radiation damage in silicon from the viewpoint of a machine learning interatomic potential. *Phys. Rev. Mater.* **2021**, *5*, 114603. [CrossRef]
- 28. Barberoa, N.; Forneris, J.; Grilj, V.; Jakšić, M.; Räisänen, J.; Simon, A.; Skukan, N.; Vittone, E. Degradation of the charge collection efficiency of an n-type Fz silicon diode subjected to MeV proton irradiation. *Nucl. Instrum. Methods Phys. Res. Sect. B* **2015**, 348, 260. [CrossRef]